



Title	An Extremely Porous Hydrogen-Bonded Framework Composed of D-Penicillaminato $\text{Co}^{\text{III}}_2\text{Au}^{\text{I}}_3$ Complex Anions and Aqua Cobalt(II) Cations : Formation and Stepwise Structural Transformation
Author(s)	Surinwong, Sireenart; Yotnoi, Bunlawee; Yoshinari, Nobuto et al.
Citation	Chemistry : An Asian Journal. 2016, 11(4), p. 486-490
Version Type	AM
URL	<a href="https://hdl.handle.net/11094/57154">https://hdl.handle.net/11094/57154</a>
rights	
Note	

*The University of Osaka Institutional Knowledge Archive : OUKA*

<https://ir.library.osaka-u.ac.jp/>

The University of Osaka

# **An Extremely Porous Hydrogen-Bonded Framework Composed of D-Penicillaminato Co<sup>III</sup><sub>2</sub>Au<sup>I</sup><sub>3</sub> Complex Anions and Aqua Cobalt(II) Cations: Formation and Stepwise Structural Transformation**

Sireenart Surinwong,<sup>[a]</sup> Nobuto Yoshinari,<sup>[a]</sup> Bunlawee Yotnoi,<sup>[a,b]</sup> and Takumi Konno\*<sup>[a]</sup>

[a] S. Surinwong, Dr. N. Yoshinari, Dr. B. Yotnoi, Prof. T. Konno

Department of Chemistry, Graduate School of Science

Osaka University

Toyonaka, Osaka 560-0043 (Japan)

E-mail: konno@chem.sci.osaka-u.ac.jp

[b] Dr. B. Yotnoi,

On leave from Department of Chemistry, School of Science

University of Phayao, Phayao 56000 (Thailand)

Supporting information for this article is available on the WWW under <http://dx.doi.org/10.1002/asia.201xxxxxx>.

**Abstract:** A unique example of a hydrogen-bonded ionic solid with a porosity of 80%,  $[\text{Co}(\text{H}_2\text{O})_6]_3[\text{Co}_2\text{Au}_3(\text{D-pen-}N,S)_6]_2$  (**1**; D-H<sub>2</sub>pen = D-penicillamine), composed of  $[\text{Co}(\text{H}_2\text{O})_6]^{2+}$  cations and  $[\text{Co}_2\text{Au}_3(\text{D-pen-}N,S)_6]^{3-}$  anions, is reported. Solid **1** was kinetically produced and was then transformed stepwise into two more thermodynamically stable solids with lower porosities,  $[\text{Co}(\text{H}_2\text{O})_4][\text{Co}(\text{H}_2\text{O})_6]_2[\text{Co}_2\text{Au}_3(\text{D-pen-}N,S)_6]_2$  (**2**) and  $[\text{Co}(\text{H}_2\text{O})_4]_3[\text{Co}_2\text{Au}_3(\text{D-pen-}N,S)_6]_2$  (**3**), through the coordination of the free carboxylate groups in  $[\text{Co}_2\text{Au}_3(\text{D-pen-}N,S)_6]^{3-}$  to  $\text{Co}^{\text{II}}$  centers. Solids **1-3** were structurally characterized, and the selective adsorption of small molecules into their pores was investigated.

Porous ionic solids, in which discrete cations and anions are arranged in a crystal lattice with large inter-ionic spaces, have attracted considerable attention as a new class of porous materials.<sup>[1]</sup> This is because these compounds, which exhibit strong electrostatic interactions on internal surfaces, are easily reproduced by crystallization. The use of nanometer-sized discrete ions, such as polyoxometalates and S-bridged multinuclear metal clusters,<sup>[2,3]</sup> as components is a simple approach for the synthesis of this class of compounds that automatically expand their intermolecular spaces. However, so far, the highest reported porosities have been limited to ~50%, mainly due to the closely packed arrangement of their spherically shaped ionic components. An alternative approach, in which the connectivity numbers among cationic and anionic species are decreased through directionally controlled hydrogen-bonding interactions, has been proposed for the synthesis of highly porous ionic frameworks.<sup>[4]</sup> With this approach, ionic framework porosities of up to 63% have been reported for  $[\text{Co}(\text{H}_2\text{bim})_3](\text{TMA})$  ( $\text{H}_2\text{bim}$  = 2,2'-biimidazol;  $\text{H}_3\text{TMA}$  = 1,3,5-benzenetricarboxylic acid), in which the planar  $\text{TMA}^{3-}$  anions are hydrogen-bonded with the  $[\text{Co}(\text{H}_2\text{bim})_3]^{3+}$  cations, thus forming a 2D sheet-like structure with a 3-connected net.<sup>[5]</sup> Although the porosity of 63% is higher than that expected for the 6-connected primitive lattice (48%) and is comparable with that for the 4-connected diamondoid lattice (66%),<sup>[6]</sup> it is still lower than the porosity values found in several highly porous metal organic frameworks (MOFs) formed by coordination bonds between metal ions and organic or inorganic ligands.<sup>[7]</sup>

Studies of MOFs chemistry have established that a kinetic product is quickly formed through an accelerating polymerization process under dense reaction conditions and tends to have a more porous structure compared with the compounds produced *via* thermodynamic processes.<sup>[8]</sup> This is simply explained by the lower stability of the more highly porous structures compared with the structures with lower porosity values. Here, we report that this concept is applicable to the synthesis of an ionic solid with a porosity of 80%,  $[\text{Co}(\text{H}_2\text{O})_6]_3[\text{Co}_2\text{Au}_3(\text{D-pen-N,S})_6]_2$  (**1**; D- $\text{H}_2\text{pen}$  = D-penicillamine), in which rod-shaped  $\text{Co}^{\text{III}}_2\text{Au}^{\text{I}}_3$  complex anions,  $[\text{Co}_2\text{Au}_3(\text{D-pen-N,S})_6]^{3-}$ ,<sup>[9]</sup> are alternately hydrogen-bonded with  $[\text{Co}(\text{H}_2\text{O})_6]^{2+}$  cations to form a 3D structure with a 3-connected net. This compound was kinetically produced and isolated in the form of X-ray quality crystals from an aqueous solution containing  $[\text{Co}_2\text{Au}_3(\text{D-pen-N,S})_6]^{3-}$  and  $[\text{Co}(\text{H}_2\text{O})_6]^{2+}$ . To the best of our knowledge, such a high porosity has not been found in ionic solids consisting of cationic and anionic species without the formation of coordination bonds. As shown in Scheme 1, remarkably, the crystals **1** were transformed stepwise into two types of X-ray quality crystals,  $[\text{Co}(\text{H}_2\text{O})_4][\text{Co}(\text{H}_2\text{O})_6]_2[\text{Co}_2\text{Au}_3(\text{D-pen-N,S})_6]_2$  (**2**) and  $[\text{Co}(\text{H}_2\text{O})_4]_3[\text{Co}_2\text{Au}_3(\text{D-pen-N,S})_6]_2$  (**3**) which are thermodynamically metastable and stable products with porosities of ~60% and ~30%, respectively.

The extremely porous and highly water-soluble ionic solid **1**, was obtained in the form of purple hexagonal platelet crystals from a highly concentrated aqueous solution containing

$\text{Na}_3[\text{Co}_2\text{Au}_3(\text{D-pen-}N,S)_6]$  and  $\text{Co}(\text{OAc})_2$  in a 1:2 ratio.<sup>[10]</sup> The crystallization of **1** occurred within 12 h with a yield of ca. 40%. The electronic absorption spectrum of **1** in water shows the characteristic *d-d* transition band at 560 nm and its CD spectrum shows negative and positive bands from a shorter wavelength in this region of the spectrum (Figure S1).<sup>[10]</sup> These spectral features are the same as those for  $\text{Na}_3[\text{Co}_2\text{Au}_3(\text{D-pen-}N,S)_6]$ , indicating that **1** is composed of  $[\text{Co}_2\text{Au}_3(\text{D-pen-}N,S)_6]^{3-}$  anionic building blocks. X-ray fluorescence spectrometry implied that **1** contains Co and Au atoms, and its elemental analysis data were in good agreement with the formula for a 2:3 adduct of  $[\text{Co}_2\text{Au}_3(\text{D-pen-}N,S)_6]^{3-}$  and  $\text{Co}^{2+}$ . The presence of a high-spin octahedral  $\text{Co}^{2+}$  species in **1** in this ratio was supported by the magnetic susceptibility measurement with the observed  $\chi_{\text{M}}T$  value at 300 K of  $8.87 \text{ cm}^3 \text{ K mol}^{-1}$  and the *g* value of 2.51 (Figure S2).<sup>[10]</sup> The IR spectrum of **1** displays an intense  $\nu(\text{C}=\text{O})$  band at  $1609 \text{ cm}^{-1}$  (Figure S3),<sup>[10]</sup> indicative of the deprotonation of the D-pen carboxyl groups in **1**.<sup>[11]</sup>

The structure of **1** was established by single-crystal X-ray analysis.<sup>[12]</sup> Crystal **1** consists of rod-shaped  $[\text{Co}_2\text{Au}_3(\text{D-pen-}N,S)_6]^{3-}$  anions and octahedral  $[\text{Co}(\text{H}_2\text{O})_6]^{2+}$  cations in addition to the water molecules of crystallization.<sup>[13]</sup> The overall structure of the entire complex anion in **1** is nearly the same as that of  $\text{Na}_3[\text{Co}_2\text{Au}_3(\text{D-pen-}N,S)_6]$ ,<sup>[9]</sup> in which two  $\Lambda$ - $[\text{Co}(\text{D-pen-}N,S)_3]^{3-}$  octahedral units with free  $\text{COO}^-$  groups are linked by three linear  $\text{Au}^{\text{I}}$  ions through sulfur bridges. In **1**,  $[\text{Co}(\text{H}_2\text{O})_6]^{2+}$  cations and  $[\text{Co}_2\text{Au}_3(\text{D-pen-}N,S)_6]^{3-}$  anions are alternately arranged and thus form  $\text{OH}_2 \cdots \text{OOC}$  hydrogen bonds with an average  $\text{O} \cdots \text{O}$  distance of 2.84 Å; each  $[\text{Co}(\text{H}_2\text{O})_6]^{2+}$  cation is surrounded by three  $[\text{Co}_2\text{Au}_3(\text{D-pen-}N,S)_6]^{3-}$  anions in a right-handed skewed form, whereas each complex anion is surrounded by four  $[\text{Co}(\text{H}_2\text{O})_6]^{2+}$  cations (Figure S4).<sup>[10]</sup> As a result, a three-dimensional, 3-connected net consisting of 10-membered rings composed of ten  $[\text{Co}(\text{H}_2\text{O})_6]^{2+}$  cations as nodes and ten  $[\text{Co}_2\text{Au}_3(\text{D-pen-}N,S)_6]^{3-}$  anions as edges, is constructed (Figures 1b and 1c). This 3-connected net exhibits large opening channels with a maximum diameter of 35 Å in all directions,<sup>[14]</sup> giving an extremely high porosity of 80%, as calculated by PLATON.<sup>[15]</sup> The homogeneity of the bulk sample **1** was confirmed by powder X-ray diffraction (PXRD); the obtained diffraction pattern matched the simulated pattern calculated based on the single-crystal X-ray data (Figure S5).<sup>[10]</sup>

To check the stability of the porous structure in **1**, platelet crystals **1** (Figure 2a) were stored in a mother liquor for several days in a closed vessel. A change in the crystal shape was clearly noticed after 5 days with the appearance of block crystals **2** (Figure 2b). When the soaking time was extended to 7 days, a second change in the crystal shape was observed with the appearance of needle crystals **3** (Figure 2c). The PXRD investigation (Figure 2d) showed that a pure phase of **1** was retained for 3 days in a mother liquor with the subsequent transformation to a pure phase of **2** after 5 days and then to a pure phase of **3** after 7 days.<sup>[16]</sup>

The structures of **2** and **3** were also determined by single-crystal X-ray analysis. Crystal **2** contains *trans*-[Co(H<sub>2</sub>O)<sub>4</sub>]<sup>2+</sup> cations, each of which connects two [Co<sub>2</sub>Au<sub>3</sub>(D-pen-*N,S*)<sub>6</sub>]<sup>3-</sup> anions, and isolated [Co(H<sub>2</sub>O)<sub>6</sub>]<sup>2+</sup> cations, in addition to the water molecules of crystallization (Figure 1d).<sup>[12,13]</sup> In **2**, the [Co<sub>2</sub>Au<sub>3</sub>(D-pen-*N,S*)<sub>6</sub>]<sup>3-</sup> anions are hydrogen-bonded to each other (av. N···O = 2.92 Å), thus forming a six-fold helix with right handedness along the *c* axis. In addition, the two helices are bridged by the *trans*-[Co(H<sub>2</sub>O)<sub>4</sub>]<sup>2+</sup> cations through coordination bonds (av. Co–OOC = 2.05 Å), resulting in a double helix structure with a large 1D pore with a diameter of ca. 18 Å (Figure 1e). The double helices are further connected by [Co<sub>2</sub>Au<sub>3</sub>(D-pen-*N,S*)<sub>6</sub>]<sup>3-</sup> anions through NH<sub>2</sub>···OOC hydrogen bonds (av. N···O = 2.92 Å), completing a 1D channel structure with a porosity of ~60% (Figures 1f and S6).<sup>[10]</sup> This 1D channel structure is sustained by the [Co(H<sub>2</sub>O)<sub>6</sub>]<sup>2+</sup> cations, each of which is hydrogen-bonded to the two [Co<sub>2</sub>Au<sub>3</sub>(D-pen-*N,S*)<sub>6</sub>]<sup>3-</sup> anions in the double-helix and one [Co<sub>2</sub>Au<sub>3</sub>(D-pen-*N,S*)<sub>6</sub>]<sup>3-</sup> anion that connects the double-helix (av. O···O = 2.72 Å). The connecting mode of the three [Co<sub>2</sub>Au<sub>3</sub>(d-pen-*N,S*)<sub>6</sub>]<sup>3-</sup> anions by each [Co(H<sub>2</sub>O)<sub>6</sub>]<sup>2+</sup> cation is the same as that found in **1** (Figure S7).<sup>[10]</sup> On the other hand, **3** does not have isolated [Co(H<sub>2</sub>O)<sub>6</sub>]<sup>2+</sup> cations, but contains the *cis*- and *trans*-[Co(H<sub>2</sub>O)<sub>4</sub>]<sup>2+</sup> cations that are directly bound to [Co<sub>2</sub>Au<sub>3</sub>(D-pen-*N,S*)<sub>6</sub>]<sup>3-</sup> anions (Figures 1g and S8).<sup>[10]</sup> In **3**, [Co<sub>2</sub>Au<sub>3</sub>(D-pen-*N,S*)<sub>6</sub>]<sup>3-</sup> anions are alternately connected by the *cis*-[Co(H<sub>2</sub>O)<sub>4</sub>]<sup>2+</sup> cations through coordination bonds (av. Co–OOC = 2.06 Å), forming a 2-fold helix along the *b* axis. In addition, the two helices are connected to each other through OH<sub>2</sub>···OOC hydrogen bonds (av. O···O = 2.86 Å), thus forming a right-handed double helix structure (Figures 1h and S9).<sup>[10]</sup> The double helices are connected by the *trans*-[Co(H<sub>2</sub>O)<sub>4</sub>]<sup>2+</sup> cations through coordination bonds (av. Co–OOC = 2.03 Å) in a 2D sheet-like structure. Finally, the 2D sheets are stacked through the NH<sub>2</sub>···OOC and OH<sub>2</sub>···OOC hydrogen bonds (av. N···O = 3.01 Å, O···O = 2.69 Å), completing a 3D dense structure with a low porosity of ~30% (Figure 1i).

The structural conversions from **1** to **2** and to **3** imply that **1** is a kinetic product, whereas **2** and **3** are thermodynamically metastable and stable products, respectively. The connectivity between the cations and anions indicates that **1** contains only the hydrogen bonds between [Co(H<sub>2</sub>O)<sub>6</sub>]<sup>2+</sup> and [Co<sub>2</sub>Au<sub>3</sub>(D-pen-*N,S*)<sub>6</sub>]<sup>3-</sup>. In contrast, **2** contains coordination bonds between [Co(H<sub>2</sub>O)<sub>4</sub>]<sup>2+</sup> and [Co<sub>2</sub>Au<sub>3</sub>(D-pen-*N,S*)<sub>6</sub>]<sup>3-</sup> in addition to the hydrogen bonds between [Co(H<sub>2</sub>O)<sub>6</sub>]<sup>2+</sup> and [Co<sub>2</sub>Au<sub>3</sub>(D-pen-*N,S*)<sub>6</sub>]<sup>3-</sup>, with only coordination bonds between [Co(H<sub>2</sub>O)<sub>4</sub>]<sup>2+</sup> and [Co<sub>2</sub>Au<sub>3</sub>(D-pen-*N,S*)<sub>6</sub>]<sup>3-</sup> involved in **3**. Thus, the kinetic product of **1** is converted to the thermodynamic product **3**, by way of **2**, through the replacement of hydrogen bonds by coordination bonds that have a greater binding energy.<sup>[17]</sup> We note that **2** reverted back to **1** by the dissolution and the subsequent crystallization procedures. This is a substantial advantage for the ionic solids over the MOFs that are commonly insoluble in solution and thus are not reproducible.

To investigate the adsorption characteristics of **1**, **2**, and **3** toward small molecules, their adsorption isotherms for H<sub>2</sub>O, EtOH, and acetone vapors were measured at 298 K. As shown in Figure 3, a remarkably high H<sub>2</sub>O adsorption capacity was observed for **1** with a value of 45 mol/mol at  $P/P_0 = 0.90$ . A clear hysteresis loop was observed in an adsorption–desorption cycle for **1**, indicative of the strong host-guest interactions accompanied by a structural transformation during the adsorption process.<sup>[18]</sup> Although a similar H<sub>2</sub>O adsorption isotherm with a clear hysteresis loop was observed for **2**, the adsorption amount (38 mol/mol at  $P/P_0 = 0.99$ ) was smaller, consistently with its lower porosity (Figure S10). The amount of adsorbed H<sub>2</sub>O was further decreased (14 mol/mol at  $P/P_0 = 0.96$ ) for **3** with no hysteresis loop obtained because of its rigid framework with a low porosity (Figure S11). Remarkably, all three compounds (**1**, **2** and **3**) showed no appreciable adsorption capability toward EtOH and acetone vapors (Figures 3, S10, and S11),<sup>[10]</sup> This is attributed to the super-hydrophilic character of their opening channels,<sup>[19]</sup> surrounded not only by the amine and carboxylate groups of D-pen but also by the aqua groups in [Co(H<sub>2</sub>O)<sub>6</sub>]<sup>2+</sup>. The adsorption isotherms for CO<sub>2</sub> and N<sub>2</sub> gases were also measured. The CO<sub>2</sub> adsorption isotherm for **1** at 195 K displayed a gradual increase and reached a value of 18.0 cm<sup>3</sup>/g at  $P/P_0 = 0.96$  (Figure S12).<sup>[10]</sup> Similar CO<sub>2</sub> adsorption isotherms were observed for **2** and **3**, but the adsorption amounts decreased in parallel with the decrease in their porosities (Figures S13 and S14).<sup>[10]</sup> In contrast, the adsorption capacities of N<sub>2</sub> gas for **1**, **2**, and **3** are all poor at 77 K (<2.4 cm<sup>3</sup>/g), reflecting the super-hydrophilic character of its porous structure.

In summary, we showed that the use of [Co<sub>2</sub>Au<sub>3</sub>(D-pen-*N,S*)<sub>6</sub>]<sup>3-</sup> as an anionic species and [Co(H<sub>2</sub>O)<sub>6</sub>]<sup>2+</sup> as a cationic species leads to the creation of an ionic solid (**1**) with an extremely high porosity of 80%, in which the cationic and anionic species are alternately linked solely by COO⋯HO hydrogen bonds. This is due to the presence of terminal, non-coordinating carboxylate groups in the rod-shaped, chiral complex anion that forms skewed, 3-connected hydrogen bonds around the aqua groups in the octahedral [Co(H<sub>2</sub>O)<sub>6</sub>]<sup>2+</sup>. Compound **1** was transformed stepwise to the thermodynamically more stable solids with denser structures, **2** and **3**, induced by the coordination of the carboxylate groups to the Co<sup>II</sup> centers. Such a stepwise transformation, in which all the three solid phases are crystallographically characterized, is quite rare. In addition, the selective high capture of H<sub>2</sub>O over EtOH or acetone, together with that of CO<sub>2</sub> over N<sub>2</sub>, was recognized especially for **1**, which is ascribed to its porous ionic structures with super-hydrophilic opening channels. Attempts to accommodate large, chiral hydrophilic molecules are currently underway in our laboratory.

## Experimental Section

Experimental details, together with spectroscopic, crystallographic, magnetic, and adsorption data, are given in the Supporting Information.

## Acknowledgements

This work was supported by CREST, JST and Grants-in-Aids for Science Research (No. 25870387 and 15K21127) from the Ministry of Education, Culture Sports, Science and Technology of Japan. The synchrotron radiation experiments were performed at the BL02B1 and BL02B2 of SPring-8 with the approval of the Japan Synchrotron Radiation Research Institute (JASRI) (Proposal No. 2014B1021, 2015A1506, 2015A1520). We thank Prof. Masaki Kawano and Dr. Tatsuhiko Kojima (POSTECH) for assisting with the single-crystal X-ray measurement at the 2D beamline in the Pohang Accelerator Laboratory supported by POSTECH. Mr. Yoshinari Kurioka (Osaka University) is also acknowledged for his experimental support.

## References

- [1] a) S. Uchida, N. Mizuno, *Coord. Chem. Rev.* **2007**, *251*, 2537-2546; b) S. Takamizawa, T. Akatsuka, T. Ueda, *Angew. Chem., Int. Ed.* **2008**, *47*, 1689-1692; *Angew. Chem.* **2008**, *120*, 1713-1716.
- [2] a) S. Uchida, M. Hashimoto, N. Mizuno, *Angew. Chem., Int. Ed.* **2002**, *41*, 2814-2817; *Angew. Chem.* **2002**, *114*, 2938-2941; b) K. Suzuki, Y. Kikukawa, S. Uchida, H. Tokoro, K. Imoto, S. Ohkoshi, N. Mizuno, *Angew. Chem., Int. Ed.* **2012**, *51*, 1597-1601; *Angew. Chem.* **2012**, *124*, 1629-1633; c) R. Eguchi, S. Uchida, N. Mizuno, *Angew. Chem., Int. Ed.* **2012**, *51*, 1635-1639; *Angew. Chem.* **2012**, *124*, 1667-1671; d) R. Kawahara, S. Uchida, N. Mizuno, *Inorg. Chem.* **2014**, *53*, 3655-3661; e) R. Kawahara, S. Uchida, N. Mizuno, *Chem. Mater.* **2015**, *27*, 2092-2099.
- [3] a) N. Yoshinari, K. Tatsumi, A. Igashira-Kamiyama, T. Konno, *Chem. Eur. J.* **2010**, *16*, 14252-14255; b) N. Yoshinari, U. Yamashita, T. Konno, *CrystEngComm* **2013**, *15*, 10016-10019.
- [4] a) M. Tadokoro, J. Toyoda, K. Isobe, T. Itoh, A. Miyazaki, T. Enoki, K. Nakasuji, *Chem. Lett.* **1995**, *24*, 613-614; b) M. Tadokoro, K. Isobe, H. Uekusa, Y. Ohashi, J. Toyoda, K. Tashiro, K. Nakasuji, *Angew. Chem., Int. Ed.* **1999**, *38*, 95-98; *Angew. Chem.* **1999**, *111*, 102-106; c) M. Tadokoro, K. Nakasuji, *Coord. Chem. Rev.* **2000**, *198*, 205-218; d) M. Tadokoro, H. Kanno, T. Kitajima, H. S. Umemoto, N. Nakanishi, K. Isobe, K. Nakasuji, *Proc. Natl. Acad. Sci. U. S. A.* **2002**, *99*, 4950-4955; e) M. Tadokoro, Y. Tanaka, K. Noguchi, T. Sugaya, K. Isoda, *Chem. Commun.* **2012**, *48*, 7155-7157.



- [5] M. Tadokoro, S. Fukui, T. Kitajima, Y. Nagao, S. Ishimaru, H. Kitagawa, K. Isobe, K. Nakasuji, *Chem. Commun.* **2006**, 1274-1276.
- [6] a) P. Krishna, D. Pandey, *Close-Packed Structures*, University College Cardiff Press, Cardiff, Wales, **1981**; b) L. E. Smart, E. A. Moore, *Solid State Chemistry: An Introduction* (Fourth edition), CRC Press, Boca Raton, Florida, **2012**.
- [7] a) H. Furukawa, N. Ko, Y. B. Go, N. Aratani, S. B. Choi, E. Choi, A. O. Yazaydin, R. Q. Snurr, M. O'Keeffe, J. Kim, O. M. Yaghi, *Science* **2010**, 329, 424-428; b) H. Furukawa, K. E. Cordova, M. O'Keeffe, O. M. Yaghi, *Science* **2013**, 341, 974-986; c) I. Senkovska, S. Kaskel, *Chem. Commun.* **2014**, 50, 7089-7098.
- [8] a) S. H. Jhung, J. H. Lee, P. M. Forster, G. Férey, A. K. Cheetham, J. S. Chang, *Chem. Eur. J.* **2006**, 12, 7899-7905; b) M. Kawano, T. Haneda, D. Hashizume, F. Izumi, M. Fujita, *Angew. Chem., Int. Ed.* **2008**, 47, 1269-1271; *Angew. Chem.* **2008**, 120, 1289-1291; c) J. Martí-Rujas, M. Kawano, *Acc. Chem. Res.* **2013**, 46, 493-505.
- [9] T. Konno, A. Toyota, A. Igashira-Kamiyama, *J. Chin. Chem. Soc.* **2009**, 56, 26-33.
- [10] For detailed information on preparation procedures and characterization data, please see the Supporting Information.
- [11] K. Nakamoto, *Infrared and Raman Spectra of Inorganic and Coordination Compounds*, Wiley, New York, **1997**.
- [12] CCDC 1436194, 1436195, 1436559 contain the supplementary crystallographic data for **1**, **2**, and **3**. These data can be obtained free of charge from The Cambridge Crystallographic Data Centre.
- [13] A part of  $[\text{Co}(\text{H}_2\text{O})_6]^{2+}$  cations in **1** and **2** could not be modeled in the crystal structure, presumably due to the severe disorder in the large void space.
- [14] A large number of solvated water molecules, which should be present in the large void space, are removed easily even at room temperature, resulting in a decrease of framework crystallinity in air.
- [15] A. L. Spek, *J. Appl. Cryst.* **2003**, 36, 7-13.
- [16] Compounds **2** and **3** were fully characterized by absorption, CD, and IR spectroscopies, as well as elemental, fluorescence X-ray, SQUID, and powder X-ray diffraction analyses.<sup>[10]</sup>
- [17] G. R. Desiraju, T. Steiner, *The Weak Hydrogen Bond in Structural Chemistry and Biology*, Oxford University Press, Oxford, **1999**.
- [18] a) J. Canivet, J. Bonnefoy, C. Daniel, A. Legrand, B. Coasne, D. Farrusseng, *New J. Chem.* **2014**, 38, 3102-3111; b) J. Canivet, A. Fateeva, Y. Guo, B. Coasne, D. Farrusseng, *Chem. Soc. Rev.* **2014**, 43, 5594-5617; c) N. C. Burtch, H. Jasuja, K. S. Walton, *Chem. Rev.* **2014**, 114, 10575-10612.

- [19] a) A. Nalaparaju, X. S. Zhao, J. W. Jiang, *J. Phys. Chem. C* **2010**, *114*, 11542-11550; b) R. Plessius, R. Kromhout, A. L. D. Ramos, M. Ferbinteanu, M. C. Mittelmeijer-Hazeleger, R. Krishna, G. Ronthenberg, S. Tananse, *Chem. Eur. J.* **2014**, *20*, 7922-7925; c) J. J. Gutiérrez-Sevillano, S. Calero, R. Krishna, *J. Phys. Chem. C* **2015**, *119*, 3658-3666.

## Scheme and figure legends

### Scheme 1.

Stepwise conversion from **1** to **3** via **2**. Dashed lines represent COO...HO hydrogen bonds.

### Figure 1.

a) Perspective views of the expanded asymmetric unit, b) a 10-membered ring, and c) a 3D hydrogen-bonded framework in **1**. d) Perspective views of the expanded asymmetric unit, e) two double helices (purple and orange) connected by  $[\text{Co}_2\text{Au}_3(\text{D-pen-}N,S)_6]^{3-}$  anions (white), f) a 1D channel structure in **2**. g) Perspective views of expanded asymmetric unit, h) two double helices (purple and orange) connected by *trans*- $[\text{Co}(\text{H}_2\text{O})_4]^{2+}$  units, and i) a 3D dense structure with 2D coordination polymers in **3**. Color codes:  $\text{Co}^{\text{II}}$ , light blue;  $\text{Co}^{\text{III}}$ , purple; Au, gold; S, yellow; O, pink; N, blue; C, gray.

### Figure 2.

Images of crystals a) **1**, b) **2**, and c) **3**. d) PXRD patterns showing structural conversion of **1** in its mother liquor. Patterns observed at 4 and 6 days matched well with the mixture of **1** & **2** and **2** & **3**, respectively.

### Figure 3.

Vapor adsorption (solid symbols) and desorption (open symbols) isotherms of **1** for  $\text{H}_2\text{O}$  (black), EtOH (blue), and acetone (red) at 298 K.

## Scheme and figures

### Scheme 1.

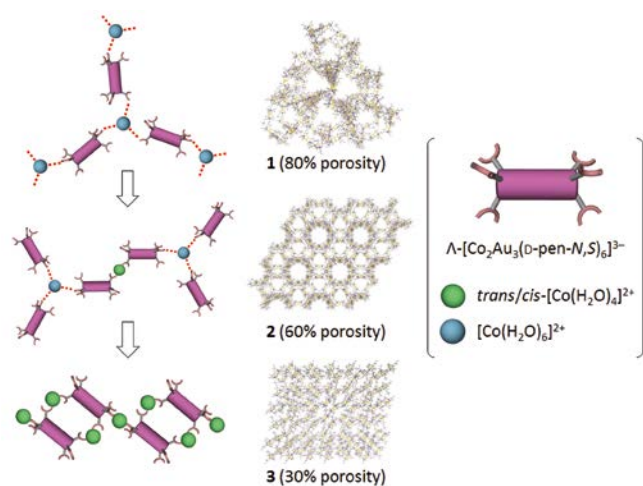
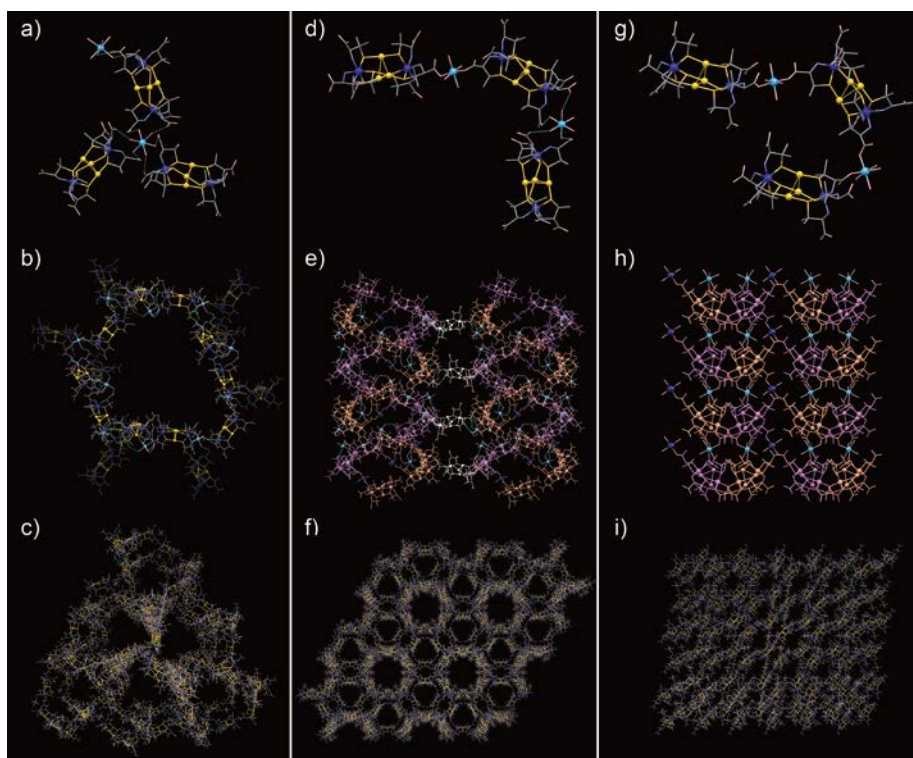
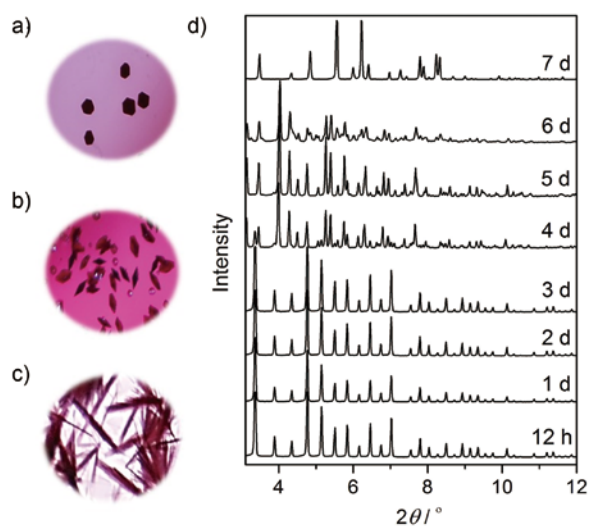


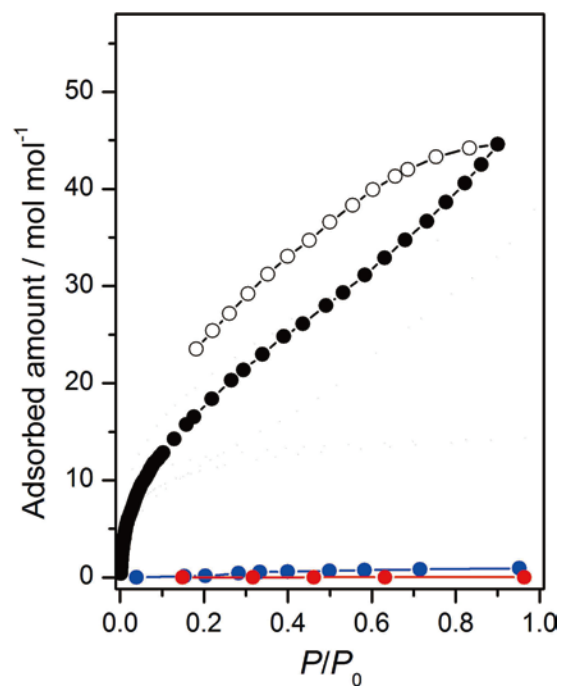
Figure 1.



**Figure 2.**



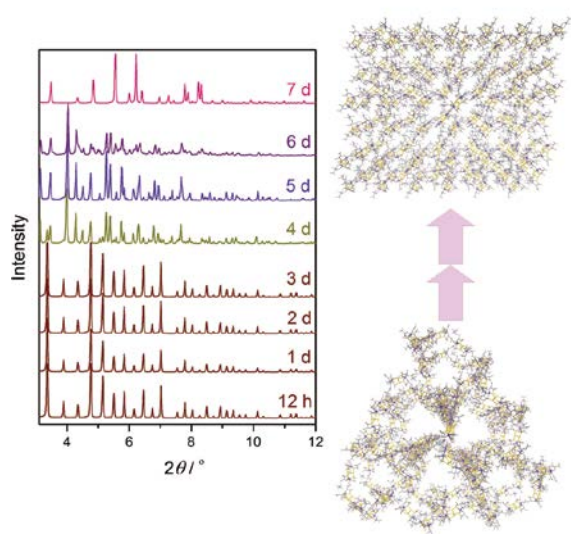
**Figure 3.**



### Text for the Table of Contents

A hydrogen-bonded ionic solid composed of aqua cobalt(II) cations and  $\text{Co}^{\text{III}}_2\text{Au}^{\text{I}}_3$  complex anions, which exhibits the highest-ever porosity of 80%, was kinetically produced and was stepwise transformed to two thermodynamically stable solids with lower porosities. This compound showed selective, high adsorption of  $\text{H}_2\text{O}$  over EtOH and  $\text{CO}_2$  over  $\text{N}_2$ , which is ascribed to its super-hydrophilic porous structure.

### Table of Contents illustration



**Keywords**

adsorption • ionic solids • porous compounds • structural transformation • X-ray diffraction